JOURNAL OF NANO- AND ELECTRONIC PHYSICS
Vol. **6** No 1, 01004(5pp) (2014)

ЖУРНАЛ НАНО- ТА ЕЛЕКТРОННОЇ ФІЗИКИ
Том **6** № 1, 01004(5cc) (2014)

The Design of a Low Power MEMS Based Micro-hotplate Device Using a Novel Nickel Alloy for Gas Sensing Applications

Bijoy Kantha*, Subir Kumar Sarkar

Jadavpur University, 188, Raja S. C. Mullick Road, Kolkata – 700032 West Bengal, India

(Received 01 October 2013; published online 06 April 2014)

In this paper comparative analysis of MEMS (Micro-electro-mechanical System) based Micro-hotplate using three different heating elements use as separately are presented. Three different materials (viz. DilverP1, Polysilicon, and Platinum) are used as heating elements with same thickness of 0.2 μm. CoventorWare™ simulator has been used for construction of 3D model and electro-thermo-mechanical analysis of Micro-hotplate device. Power consumption, stress and displacement of Micro-hotplate are studied at operating temperature (165 °C). It is obtained that power consumption, stress and displacement of Dilverp1 heating element are 13.06 mW, 190 MPa and 0.028 μm which are less in comparison to those with Poly Silicon heater and Platinum heater at moderate temperature (150-200 °C) over the sensing material (ZnO).

Keywords: MEMS, Micro-hotplate, CoventorWare™, Electro-thermo-mechanical, ZnO.

PACS numbers: 44.10. + i, 73.50.Lw, 62.20. – x

1. INTRODUCTION

Metal oxide based Micro-hotplate devices are essential for their versatile applications in industrial and domestic activities [1]. Low power consumption is a basic requirement for a gas sensor with an acceptable battery life-time. Conventional type gas sensor had some properties like high power consumption (500 mW-1 W) and high operating temperature (≥ 300 °C) [2]. Several work on platinum and polysilicon heating element based gas sensors with high operating temperature (400-700 °C) [2] have been reported. The life time of the hotplate is reduced due to high power consumption. The problems can be reduced with the application of MEMS technology [3]. Several nano-structured semiconducting oxide based gas sensor's works have been recorded at relatively low temperature (150-300 °C) [4, 5]. The advantages of semiconductor gas sensors are low power consumption and a real simplicity in function, good mechanical stability, CMOS compatibility and low cost [6-8].Very little similar type report has been published on metal oxide based micro-hotplate device [8]. The various micromachining processes of low power MEMS micro-hotplate structure have been demonstrated [9-13].

Gas sensors based on the semiconducting metal-oxides such as SnO_2 and ZnO [14-18] have been found to be very useful for detecting ethanol vapor, oxygen [19] and H_2 [20] gases. Electro-thermo-mechanical analysis of Micro-hotplate model is determined by CoventorWare™ software (A MEMS design and simulation software). Software based simulator is used to save the cost of device fabrication. The Mem Mech solver of CoventorWare™ software is used to obtain the temperature, mechanical deflection and stress distribution of the MEMS based Micro-hotplate. The result is used to predict the temperature and displacement as a function of the applied voltage across heating layer. The mechanical behavior of the micro-hotplate is analyzed using the displacement result of the micro-hotplate. In this paper MEMS based Micro-hotplate device using different heating materials (DilverP1, Polysilicon, Platinum) is reported for the detection of suitable material as heating element which is consumed low power and ZnO is used as a sensing layer of the Micro-hotplate. It has shown that power consumption, stress and displacement of Dilverp1 material are less in comparison to those with Poly Silicon heater and Platinum heater at moderate temperature (150-200 °C) over the sensing material. So Dilverp1 heater will provide good mechanical strength comparison to those with Pt heater, Poly Silicon heater.The structure of MEMS based Micro-hotplate device is presented in section 2. Mathematical Formulations are discussed in section 3. Results and Discussions are presented in section 4 and conclusion appears in section 5.

2. DEVICE STRUCTURE

The flow chart for the preparation of the Micro-hotplate device is pictorially depicted in Fig. 1. The simulation based fabrication is initially started with deposition of glass wafer (0.5 μm) and then heater layer (DilverP1) with a length of 18μm, width of 20 μm and thickness of 5μm is deposited to glass wafer to form the anchor. After formation of the anchor, DilverP1 layer with a length of 100 μm, width of 22 μm and thickness of 0.2 μm is deposited on the anchors to form the heater layer. Silicon Nitride (Si_3N_4) and Silicon-di-oxide (SiO_2) are used as an isolation layer of Micro-hotplate device. In this design, the electrode and sensing elements are gold (Au) with the thickness of 0.3 μm and zinc oxide (ZnO) with the thickness of 0.6 μm. Gold electrodes are deposited on the ZnO layer of the Micro-hotplate device. The thicknesses of air-gap, isolation, electrode, and sensing layers are 4 μm, 1 μm respectively. The dimension of central beam is 12 μm × 14 μm. The different simulation based fabrication steps for developing the Micro-hotplate in CoventorWare™ (A MEMS design and simulation software) are stack material depo-

*bijoyvlsi@gmail.com

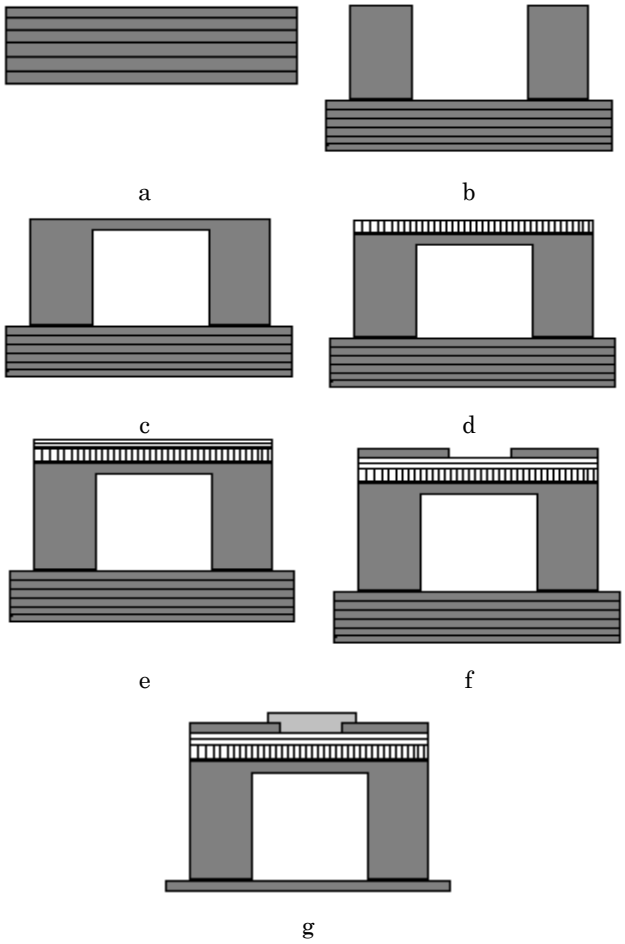

Fig. 1 – The process flow chart of the device

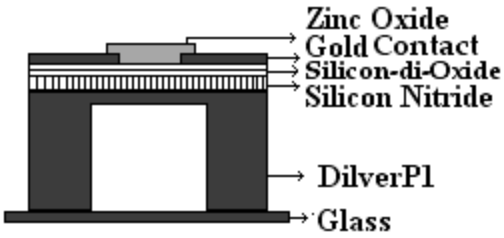

Fig. 2 – The structure of micro-hotplate device

sition, planar fill process, wet etching process, sacrificed process and photolithography.

The extruded brick mesh with lateral element size of 10 μm is selected for the solid model. The fine-structure region is consisted of Si_3N_4, Au, ZnO layers. The fine-structure region is meshed with element size of 0.3 μm. The structure of micro-hotplate device is shown in fig. 2. CoventorWare™ software has been used for the simulation of the device.

3. MATHEMATICAL FORMULATIONS

Heat is produced in Micro-hotplate and can be estimated by Joule's Law as follows

$$\Delta q = rI^2 \Delta t \tag{1}$$

Here heated-area resistance is denoted by r and Δt denotes the time in second. Thermal losses are mainly three types: conduction in the device, convection in the air and radiation. So, the generation of heat by the micro-hotplate is the combination of three heat losses (conduction q_c, convection q_{con}, and radiation q_r)

$$\Delta q = rI^2 \Delta t = q_c + q_{con} + q_r \tag{2}$$

The power can be obtained from equation (2) by dividing with time (Δt)

$$rI^2 = \frac{\Delta q_c}{\Delta t} + \frac{\Delta q_{con}}{\Delta t} + \frac{\Delta q_r}{\Delta t} \tag{3}$$

First, the power lose due to conduction in the substrate is given by

$$\frac{\Delta q_c}{\Delta t} = KA \frac{\Delta \theta}{\Delta x} \tag{4}$$

Here thermal conductivity of the substrate is denoted by K, A is the area of cross-section of the surface in the substrate and temperature gradient is denoted by $\Delta\theta / \Delta x$.

Second, the power lose due to convection in the air is defined as

$$\frac{\Delta q_{con}}{\Delta t} = h_{conv} A_{conv} . \Delta \theta \tag{5}$$

h_{conv} is the Heat transfer coefficient (assumed independent of t here) A_{conv} is the surface area of the heat being transferred, $\Delta\theta$ is the time-dependent thermal gradient between environment and device.

Third, the powers lose due to radiation is given by [21]:

$$\frac{\Delta q_r}{\Delta t} = \varepsilon \sigma S_r \Delta \theta^4 \tag{6}$$

Here the emissivity of the material is denoted by ε, σ is the Stefan-Boltzmann constant ($5.67 \times 10^{-8} \mathrm{Wm^{-2}K^{-4}}$) and the radiation of the surface is denoted by S_r. So, the total power loses can be defined by replacing the values of three power losses into equation (3):

$$rI^2 = KA \frac{\Delta \theta}{\Delta x} + h_{conv} A_{conv} \Delta \theta + \varepsilon \sigma S_r \Delta \theta^4 \tag{7}$$

The displacement is evaluated from the stress and mechanical static equation using the input thermal strain obtained from the solved temperature distribution and thermal expansion coefficient [8].

$$\delta = \mathrm{Y}(\varepsilon - \sigma_i) \tag{8}$$

$$\sigma_i = \alpha \Delta T \tag{9}$$

Where δ, ε, σ_i, Y, α, $\Delta\theta$ are stress, strain, initial thermal strain, young's modulus matrix, thermal expansion coefficient and differential temperature respectively.

4. RESULTS AND DISCUSSIONS

The parameters are used in our simulation are given in Table 1. The simulation result of temperature

distribution of Micro-hotplate with selected heater material (DilverP1) is depicted in Fig. 3. It shows from Fig. 3 that the temperature of DilverP1 plate layer is 438 K at the center of DilverP1 plate layer. Proper electrical isolation is provided by using Silicon Nitride (Si_3N_4) and Silicon-di-oxide (SiO_2) layers. SiO_2 and Si_3N_4 are used to improve the temperature uniformity above the sensing layer (ZnO). The stress distribution and mechanical deflection of Micro-hotplate using DilverP1 material are shown in Fig. 4 and in Fig. 5. The mechanical deflection of DilverP1 heating material is less than other two materials. Based on the simulation result, it is noted that maximum stress occurs at the edge regions of the Micro-hotplate. The Current Density distribution of DilverP1 is shown in Fig. 6. The stress distributions of Polysilicon and Platinum based Micro-hotplate are shown in Fig. 7 and in Fig. 8.

Table 1 – Device Parameters used in the Simulation of Micro-hotplate

Parameter	Value
Length of DilverP1 material	100 μm
Width of DilverP1 material	22 μm
Thickness of DilverP1 material	0.2 μm

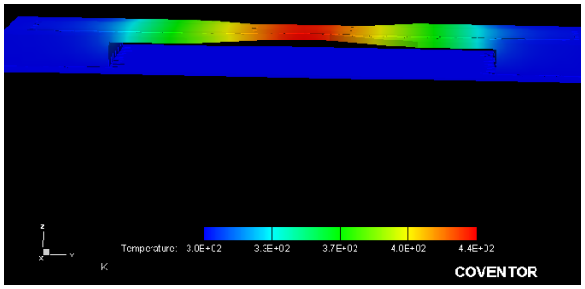

Fig. 3 – Electro-thermal simulation of 0.2 μm thick beam of DilverP1 material using CoventorWare™ Software

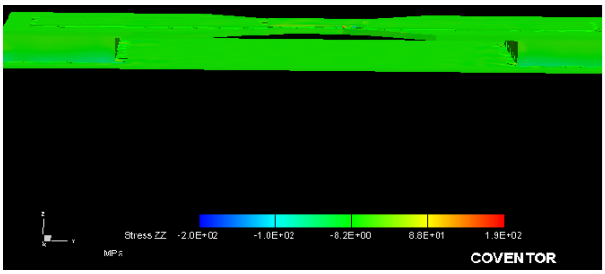

Fig. 4 – Stress distribution of 0.2 μm thick beam of DilverP1 material using CoventorWare™ Software

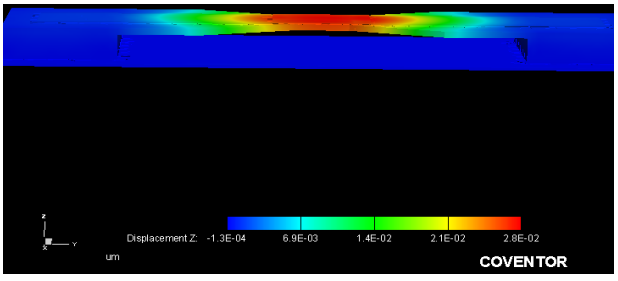

Fig. 5 – Electro-mechanical simulation of 0.2 μm thick beam of DilverP1 material using CoventorWare™ Software

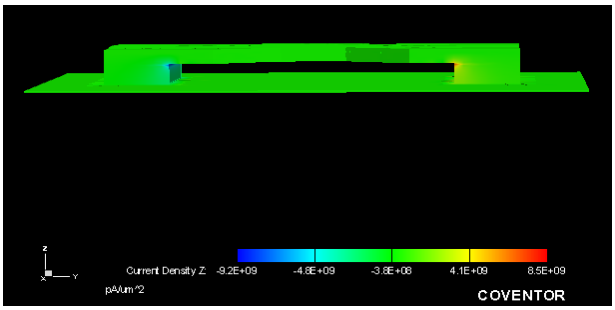

Fig. 6 – Current Density distribution of 0.2 μm thick beam of DilverP1 material using CoventorWare™ Software

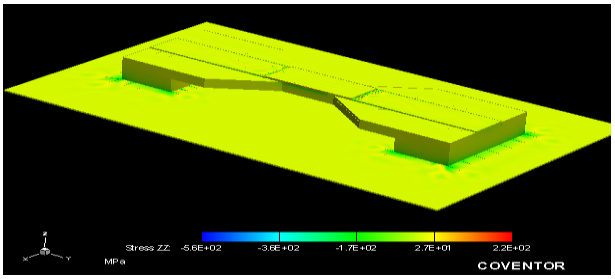

Fig. 7 – Stress distribution of 0.2 μm thick beam of Polysilicon material using CoventorWare™ Software

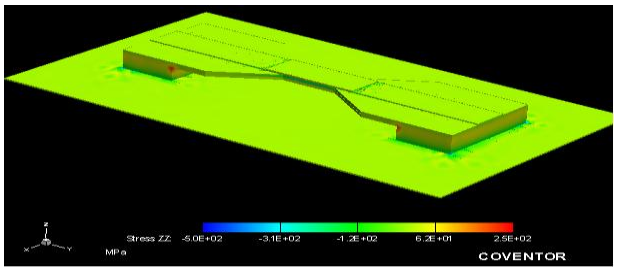

Fig. 8 – Stress distribution of 0.2 μm thick beam of Platinum material using CoventorWare™ Software

Fig. 9 indicates Power Consumption-Voltage characteristics plot of Micro-hotplate using different heating elements (DilverP1, Polysilicon, and Platinum). From Fig. 9, it has shown that power consumption of DilverP1 material is less in comparison to Poly Silicon plate and Platinum plate at moderate temperature (150-200 °C) over the sensing material (ZnO).

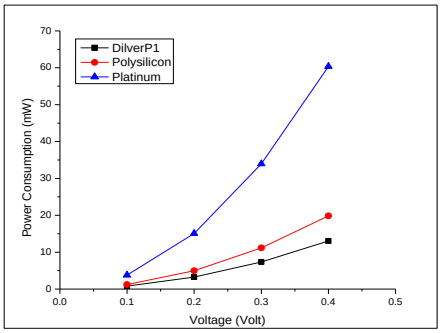

Fig. 9 – Applied voltage as a function of Power Consumption

The heater temperature along the applied voltage is plotted for different heating materials in Fig. 10. It is revealed that the temperature profile becomes more significant as applied voltage increases. Also from the

simulation results we conclude that out of the materials considered here, DilverP1 material is the best for desired operating temperature.

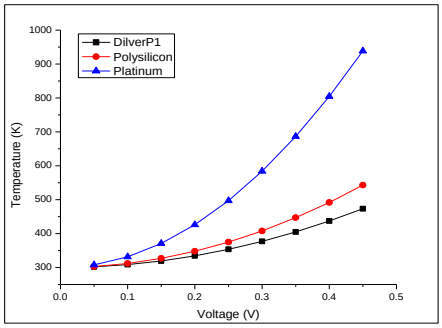

Fig. 10 – Heater Temperature-Voltage characteristics plot of Micro-hotplate device

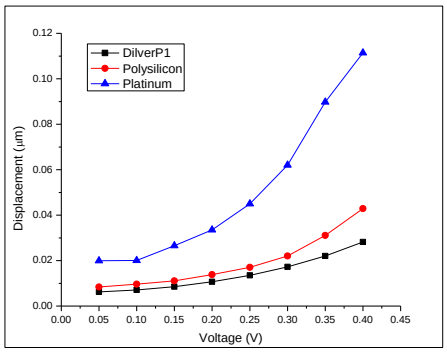

Fig. 11 – Displacement-Voltage characteristics plot of Micro-hotplate device

Fig. 11 represents the variation of displacement as a function of voltage for different heating elements (DilverP1, Polysilicon, and Platinum). From the graph, it is seen that the displacement of DilverP1 material is less than other two materials (Polysilicon plate and Platinum plate) at moderate temperature (165 °C) over the sensing material (ZnO).

This paper presents Micro-hotplate device with selected material as heating beam (DilverP1). The composition of DilverP1 is shown in Table 2 [22]. The material properties of different heating elements are given in Table 3 [22].

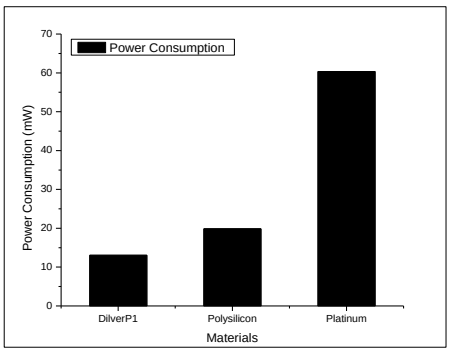

(a)

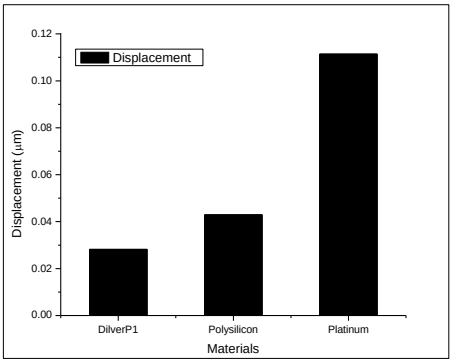

(b)

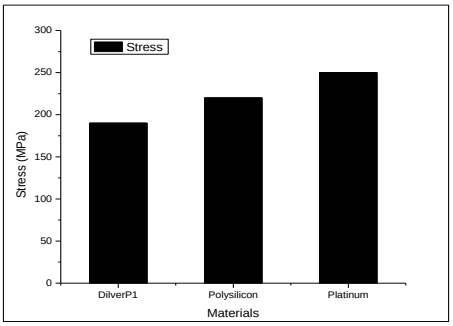

(c)

Fig. 12 – Comparison Chart (a) Power Consumption of different materials (b) Displacement of different materials (c) Stress of different materials

DilverP1 consumes low power due to high resistivity and the life time of the Micro-hotplate can be increased with the use of a low cost alloy (DilverP1) having low thermal expansion coefficient (4.2×10^{-6}/°C) and very high yield stress (680 MPa). In presence of Cobalt, DilverP1 shows corrosion resistant property. Very low stress is induced above the micro-hotplate due to low thermal expansion coefficient of DilverP1material. So it can be used as an ideal material for the micro-hotplate. The comparison chart is shown in Fig. 12. The SEM image of sensing layer is shown in Fig. 13.

Table 2 – Composition (Weight %)

Element	Ni	Co	Mn	Si	C	Fe
Typical value	29	17	≤ 0.35	≤ 0.15	≤ 0.02	Bal

Table 3 – Material Properties used in the Simulation of Micro-hotplate

Materials	Electrical resistivity in Ω·m	Young's modulus GPa
Pt	10.6×10^{-8}	168
Au	2.2×10^{-8}	78
Polysilicon	3.22×10^{-7}	169
DilverP1	49×10^{-8}	207

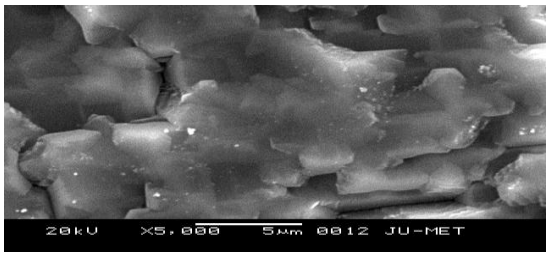

Fig. 13 – SEM image of sensing layer

5. CONCLUSION

In this paper, the electro-thermo-mechanical analysis of Micro-hotplate device has been reported at the operating temperature range of 150-200 ºC. The comparative analysis of Micro-hotplate using different heating elements ((DilverP1 micro- hotplate, Polysilicon micro-hotplate, Platinum micro hot-plate) has been presented at the same temperature (165 ºC). CoventorWare™ software is used to get temperature, displacement and stress distribution of micro-hotplate. Present simulation has shown that power consumption and displacement of Dilverp1 material are less in comparison to Poly Silicon plate and Platinum plate at moderate temperature (150-200°C) above the sensing material (ZnO). The cost of DilverP1 is less compared to Platinum and Poly-Silicon, so it's suitable for cost effective gas sensor fabrication.

AKNOWLEDGEMENTS

Authors are grateful to TEQIP PHASE-II for providing the necessary fund for carrying out this work.

REFERENCES

1. I. Simon, N. Barsan, M. Bauer, U. Weimer, *Sensor. Actuat. B* **73**, 1 (2001).
2. W. Chung, C. Shim, S. Choi, D. Lee, *Sensor. Actuat. B* **20**, 139 (1994).
3. J.S. Suehle, R.E. Cavicchi, M. Gaitan, S. Semancik, *IEEE Electron. Dev. Lett.* **14**, 118 (1993).
4. P. Nunes, E. Fortunato, A. Lopes, R. Martins, *Inter. J. Inorg. Mater.* **3**, 1129 (2001).
5. P. Bhattacharyya, P.K. Basu, H. Saha, S. Basu, *Sensor. Actuat. B* **124**, 62 (2007).
6. J. Puigcorbé, D. Vogel, B. Michel, A. Vilà, A. Grácia, C. Cané, *J. Micromech. Microeng.* **13**, 548 (2003).
7. J. Puigcorbe, A.Vila, J.Cerda, A.Cirera, I.Gracia, C. Cane, J.R. Morante, *Sensor. Actruat. A* **97-98**, 379 (2000).
8. A. Wisitsoraat, A. Tuantranont, T. Lomas, *J. Phys.* **34**, 643 (2006).
9. R.E. Cavicchi, J.S. Suehle, K.G. Kreider, B.L. Shomaker, J.A. Small, M. Gaitan, P. Chaparala, *Appl. Phys. Lett.* **66**, 812 (1995).
10. R. Cavicchi, J. Suehle, K. Kreider, M. Gaitan, *IEEE Elect. Dev. Lett.* **16**, 286 (1995).
11. F. Dimeo Jr., S. Semancik, R. Cavicchi, J. Suehle, N. Tea, M. Vaudin, J. Kelliher, *Mater. Res. Soc. Symp. Proc.* **444**, 203 (1997).
12. S. Semancik, R.E. Cavicchi, M.C. Wheeler, J.E. Tiffany, G.E. Poirier, R.M. Walton, J.S. Suehle, B. Panchapakesan, D.L. De Voe, *Sensor. Actuat. B* **77**, 579 (2001).
13. M. Afridi, A. Hefner, D. Berning, C. Ellenwood, A. Varma, B. Jacob, S. Semancik, *Solid-State Electron.* **48**, 1777 (2004).
14. B.P.J.D. Costello, R.J. Ewen, N. Guernion, N.M. Ratcliffe, *Sensor. Actuat. B* **87**, 207 (2002).
15. D.F. Paraguay, M. Miki Yoshida, J. Morales, J. Solis, L.W. Estrada, *Thin Solid Films* **373**, 137 (2000).
16. P. Ivanov, E. Llobet, X. Vilanova, J. Brezmes, J. Hubalek, X. Correig, *Sensor. Actuat. B* **99**, 201 (2004).
17. X.L. Cheng, H. Zhao, L.H. Huo, S. Gao, J.G. Zhao, *Senor. Actuat. B* **102**, 248 (2004).
18. J. Tamaki, T. Maekawa, S. Matsushima, N. Miura, N. Yamazoe, *Chem. Lett.* **3**, 477 (1990).
19. G. Sberveglieri, S. Groppelli, P. Nelli, F. Quaranta, A. Valentini, L. Vasanelli, *Sensor. Actuat. B* **7**, 747 (1992).
20. T. Yamazaki, S. Wada, T. Noma, T. Suzuki, *Sensor. Actuat B* **14**, 594 (1993).
21. J. Courbat, M. Canonica, D. Teyssieux, D. Briand, N.F. de Rooij, *J. Micromech. Microeng.* **21**, 015014 (2011).
22. S. Sinha, S. Roy, C.K. Sarkar, *Int. J. Comp. Appl.* **3**, 26 (2011).